Digital Control System of Precision Electromechanical Scanner with Elasticity

VALENTIN DROZDOV
Department of Electrical Engineering and Precision Electromechanical Systems
ITMO University
197101, Saint-Petersburg, Kronverkskij Ave., 49
RUSSIAN FEDERATION
drozdovuprint@rambler.ru

VALENTIN TOMASOV
Department of Electrical Engineering and Precision Electromechanical Systems
ITMO University
197101, Saint-Petersburg, Kronverkskij Ave., 49
RUSSIAN FEDERATION
tomasov@ets.ifmo.ru

SERGEY TUSHEV
Department of Electrical Engineering and Precision Electromechanical Systems
ITMO University
197101, Saint-Petersburg, Kronverkskij Ave., 49
RUSSIAN FEDERATION
tushev.sergei@gmail.com

Abstract: The synthesis of controller algorithm for reversible electromechanical scanner of the telescope scanning axis is discussed. Digital control system is built without intermediate stage of synthesis of analog control law. The modified procedure for the synthesis of discrete optimal control law is introduced.
Elasticity influence on static and dynamic characteristics of electromechanical scanner of the telescope scanning axis is discussed. It is shown, that the controller algorithm, which provides specified scanner behavior, could be synthesized in spite of elasticity of mechanical part of scanner.

The article provides an overview of modern optical position sensors, which are used in precision drive.

The results obtained are recommended for use in high-precision electric drives of precision observations complexes. The article may be helpful for developers of precision electric drives of telescopes and electromechanical scanners.

Key-words: electromechanical scanner, elasticity, discrete control law, precision electric drive.

1 Introduction

Nowadays terrestrial optical-electronic tools (according to tradition they are often called optical telescopes) play a major role in the detection and monitoring of space objects, especially at large distances. Undoubted and unique advantages of optical telescopes are the following:

- the ability to detect distant objects by the sun or laser illumination in the night or twilight sky,
- the ability to detect objects in the infrared wavelength range of their own thermal radiation,
- high precision determination of the angular coordinates of objects,
- possibility of obtaining optical images of space objects and high-precision photometric and spectrophotometric measurements of their optical brightness.

Telescope works at infrared wavelength range and is designed to scan space object. It is set to the mount to control the angular position of the optical axis in the space. As usually, a mount has three axes of rotation: azimuth, elevation and scanning. Scanning axis is often made in the form of electromechanical scanner. Development of these

mounts and control systems for near space observation is one of the most difficult problems of modern precision instrument making. The fact is that the mount and electromechanical control systems, solving the problem of scanning an object observed, should provide unique high quality targeting. All the elements of the design concept and its mount play an important role for such problems. Usually, mount is represented as a two-mass mechanism in the process of modeling and design of electric drives. The angular resonance frequency of the mechanism caused by the torsional deformation determines frequency bandwidth of the control system, and as a result, its performance [1-5].

The synthesis of the control algorithms usually neglects elasticity links between the motor and the load in scanning electromechanical devices, when precision and speed of scanning is not required. If electromechanical scanner is a part of telescope axis, it is necessary to get high accuracy and good dynamics of scanning process. Disregard the elasticity links may be the cause of inability to provide the required system characteristics [1] - [3].

It is necessary to get a mathematical model of the electromechanical scanner with a magnetic spring as an actuator, taking into account the elastic connection between the motor and load.

2 Position sensors

Modern optical position sensors that are used in precision electric drives have very high resolution. If the number of bits of position sensor is more than 25 bits, then minimum measured value is the angle of

$$360^\circ/(2^{25}) = 1.07 \cdot 10^{-5} \text{ degrees},$$

that is 0.039 arcseconds. This high precision allows the monitoring of space objects, such as satellites and space garbage, moving at a very low rate relative to the Earth.

Optical position sensors can be divided into two large groups – relative sensors and absolute sensors. Relative sensors have one zero reference mark against which to the current position of the axis of the telescope or electromechanical scanner is determined. Before you start it is necessary to go through the zero reference mark, otherwise the data will be unreliable and erroneous. This is an important drawback of this type of sensors. The advantage is the widely spread communication interface, which is implemented in a variety of microcontroller for motor control. [7]-[9]

Absolute encoders have a more complex scheme, as each mark is unique and has its own identification code. There are also quasi-absolute encoders that have few reference marks. To obtain reliable data from such a sensor, you must first pass through the closest to the current position mark. Absolute encoders have a more complex communication interface, if compare it with the relative sensors interface. Therefore it is often necessary to use an intermediate matching device between the sensor and microcontroller. [10], [11]

Current level of development of optical sensors ensures high precision characteristics of precision electromechanical scanners and telescopes.

3 Mathematical model

As it is known, the torque of the DC motor with a limited angle of rotation is equal to

$$M = K_i i - K_\alpha \alpha_1 \quad (1)$$

In (1) i is anchor current, α_1 is rotor angle (rotation angle of first mass), K_i is stiffness of speed-load curve or current sensitivity, K_α is stiffness of speed-load curve or current sensitivity or stiffness of magnetic spring. Opposing torque for first mass is

$$M_{op1} = J_1 \frac{d\omega_1}{dt} + c_u \delta + M_{c1} \quad (2)$$

In (2) J_1 is reduced moment of inertia of the first mass, ω_1 is rotor velocity, c_u is coefficient of flexibility between rotor and load, $\alpha_1 - \alpha_2 = \delta$ is twist angle, M_{c1} is external resistance moment, e.g. friction torque. If assemble (1) and (2), one can get

$$\frac{d\omega_1}{dt} = \frac{K_i}{J_1} i - \frac{K_\alpha}{J_1} \alpha_1 - \frac{c_u}{J_1} \delta - \frac{1}{J_1} M_{c1} \quad (3)$$

The differential equation for the twist angle is

$$\frac{d\delta}{dt} = \omega_1 - \omega_2, \quad (4)$$

where ω_2 is angular velocity.

The equation of motor wingding is

$$\frac{di}{dt} = -\frac{R}{L} i - \frac{K_e}{L} \omega + \frac{1}{L} u \quad (5)$$

In (5) R is winding resistance, L is leakage inductance of the control winding, K_e is coefficient of back EMF [4] - [6].

The moving moment of force for second mass is twist moment, and opposing torque is moment of inertial forces and external load torque, from which equation of motion of the second mass could be obtained

$$\frac{d\omega_2}{dt} = \frac{c_u}{J_2} \delta - \frac{1}{J_2} M_{c2} \quad (6)$$

In (6) J_2 is reduced moment of inertia of the second mass.

Equations (3) - (6) give the standard state-space model of electromechanical scanner with elasticity:

$$\begin{aligned} \dot{x} &= A_r x + B_r u + B_{vr} M_c \\ y &= C_r x \end{aligned} \qquad (7)$$

In some systems position sensor could be placed on the first mass, or on the second mass. Consider these two cases separately. When position sensor is on the first mass, then state vector if model (7) is equal to $x = [i\ \ \omega_1\ \ \delta\ \ \omega_2\ \ \alpha_1]$, and state-space matrices are

$$A_r = \begin{bmatrix} -\frac{R}{L} & -\frac{K_e}{L} & 0 & 0 & 0 \\ \frac{K_i}{J_1} & 0 & -\frac{c_u}{J_1} & 0 & -\frac{K_\alpha}{J_1} \\ 0 & 1 & 0 & -1 & 0 \\ 0 & 0 & \frac{c_u}{J_2} & 0 & 0 \\ 0 & 1 & 0 & 0 & 0 \end{bmatrix},$$

$$B_r = \begin{bmatrix} \frac{1}{L} \\ 0 \\ 0 \\ 0 \\ 0 \end{bmatrix},\ B_r = \begin{bmatrix} 0 & 0 \\ -\frac{1}{J_1} & 0 \\ 0 & 0 \\ 0 & \frac{1}{J_2} \\ 0 & 0 \end{bmatrix},\ M_c = \begin{bmatrix} M_{c1} \\ M_{c2} \end{bmatrix}.$$

When position sensor is on the second mass, then state vector if model (7) is equal to $x = [i\ \ \omega_1\ \ \delta\ \ \omega_2\ \ \alpha_2]$, matrix A_r is changed

$$A_r = \begin{bmatrix} -\frac{R}{L} & -\frac{K_e}{L} & 0 & 0 & 0 \\ \frac{K_i}{J_1} & 0 & -\frac{c_u + K_\alpha}{J_1} & 0 & -\frac{K_\alpha}{J_1} \\ 0 & 1 & 0 & -1 & 0 \\ 0 & 0 & \frac{c_u}{J_2} & 0 & 0 \\ 0 & 0 & 0 & 1 & 0 \end{bmatrix},$$

matrices B_r, B_{vr} and vector M_c stay same.

If position sensor is placed on the first mass, then transfer function $W_1(s) = \frac{\alpha_1(s)}{u(s)}$ is equal to

$$W_1(s) = \frac{M_1(s)}{D(s)},$$

where $M_1(s) = K_i(J_2 s^2 + c_u)$,

$$D(s) = J_1 J_2 L s^5 + J_1 J_2 R s^4 + (J_1 + J_2) R c_u s^2 +$$
$$+ (J_1 L c_u + J_2 K_i K_e + J_2 L c_u) s^3 +$$
$$+ (K_\alpha L + K_i K_e) c_u s + K_\alpha R c_u$$

If position sensor is placed on the second mass, then transfer function $W_2(s) = \frac{\alpha_2(s)}{u(s)}$ is equal to $W_2(s) = \frac{M_2(s)}{D(s)}$, where $M_2(s) = K_i c_u$.

The fundamental difference between these two cases is that if position sensor is installed on the first mass, then mathematical model of the control object contains zeros. The presence of zeros of the dynamical system can be the cause of the degeneration of the system. To assess degeneration degree of the system it is proposed to use the completeness matrix of the system. It is equal to the product of the matrices of observability and controllability:

$P_{ful} = P_{obsv} P_{ctrb}$.

This matrix is positive and semi determined. The closer the value of determinant of completeness matrix to zero, the closer the dynamical system to degeneration. Control of objects that are close to degenerate, causing some problems. In view of the foregoing in the studied case, you must give preference to installing the position sensor on the second mass. Calculations show that when sensor is installed on the first mass, than the determinant of matrix of completeness is always less than the determinant of the same matrix, when the sensor is installed on the second mass.

Anchor current and angle of rotation are measured independently from position sensor placement, therefore, measurement vector is $y = [i\ \ \alpha_p]^T$, $p = 1 \vee 2$. Measurement matrix in both cases is

$$C_r = \begin{bmatrix} 1 & 0 & 0 & 0 & 0 \\ 0 & 0 & 0 & 0 & 1 \end{bmatrix}.$$

For this reason, the order of controller synthesis does not depend on the location of the the position sensor.

Focusing on digital implementation of the controller, it is necessary to make the transition from a continuous state model (7) to the discrete model of the object

$$\begin{aligned} x_{m+1} &= A_d x_m + D_d u_m \\ y_m &= C_d x_m \end{aligned} \qquad (8)$$

In (8) $A_d = e^{A_r T}$, $B_d = \int_0^T e^{A_r (T-\tau)} u(\tau) d\tau$, $C_d = C_r$. T is controller discretization interval.

This transition can be made according to the following program of MATLAB:

```
Sc = ss(Ar, Br, Cr, 0);
Sd = c2d(Sc, T);
Ad = Sd.a;
```

```
Bd = Sd.b;
Cd = Sd.c;
```

Next is the synthesis of the optimal discrete controller that minimizes the functional:

$$J = \sum_{i=0}^{\infty}(x_m^T Q x_m + u_m^T R_1 u_m).$$

Discrete optimal control for a quadratic criterion provides the location of the eigenvalues of the closed-loop system within a circle of unit radius centered at the origin for any choice of positive definite matrices of penalty for state and control. In addition, optimal control provides large enough values of the radius of stability margins, which ensures smooth transients.

However, it is well known that there are no rules of informed choice matrices fine. It is often driven by brute force. Propose the following method to overcome this difficulty. Suppose we want to get transients of continuous object (7), which are defined by the degree of stability η. Then the roots of the characteristic equation of a discrete system consisting of a discrete controller and the object (7), must lie within a circle centered at the origin of radius $r = e^{-\eta T}$.

In order to satisfy this requirement for a discrete object (8) the auxiliary matrices are formed:

$$A_n = \frac{A_{dg}}{r},\ B_n = \frac{B_{dg}}{r}. \quad (9)$$

We choose some penalty matrix of the quadratic functional of appropriate dimension, for example $Q = 0$, $R_1 = 1$. Then the matrix of feedback obtained from the solution of the discrete Riccati equation,

```
K = dlqr(An, Bn, Qs, Rs);
```

ensures the location of the eigenvalues of the matrix (10) within a circle of unit radius.

$$F_n = A_n - B_n K \quad (10)$$

If expression (9) is substituted in (10), the following expression is obtained:

$$F_n = \frac{A_{dg}}{r} - \frac{B_{dg}}{r}K = \frac{1}{r}(A_{dg} - B_{dg}K) = \frac{1}{r}F.$$

And so, $F = rF_n$.

It is known that if matrices are associated by functional relation, the same is ratio of their eigenvalues. Hence the eigenvalues of F lie inside the circle of radius r. As a result of given admission, problem of choosing penalty matrix of the quadratic functional is replaced by the problem of choosing a number η, which has clear physical meaning and determines the system performance, $\eta = \frac{3}{t_n}$, where t_n is desired step response time.

Found feedback matrix is used in the control law,

$$u_m = -Kx_m, \quad (11)$$

which provides a specified time of the transition process in the control of the object (7).

This control (11) cannot be realized in the pure form for the reason that only two of five state variables are measured. Missing information could be obtained using a reduced discrete observer of the third order. In this case, the (11) takes the form (12).

$$u_m = N_2 w_m + N_1 y_m \quad (12)$$

In (12) $w_m = C_n x_m$ is not measured coordinates of the state of control object. Control laws (11) and (12) are equivalent in case

$$\begin{bmatrix} N_1 & N_2 \end{bmatrix} = -K\begin{bmatrix} C_d \\ T_n \end{bmatrix}^{-1}. \quad (13)$$

Unmeasured coordinates are estimated by controller by solving the real-time difference equation

$$w_{m+1} = A_n w_m + B_n u_m + R_n y_m. \quad (14)$$

In (14) A_n is arbitrary Hurwitz matrix, e.g. matrix $A_n = diag([0.1r\ \ 0.2r\ \ 0.3r])$, $B_n = C_n B_d$ matrix R_n is chosen to provide controllability of pair (A_n, R_n), e.g.,

$$R_n = \begin{bmatrix} 0 & 1 \\ 0 & 1 \\ 0 & 1 \end{bmatrix}.$$

It is also required matrix to satisfy the Sylvester equation:

$$C_n A_d - A_n C_n = R_n C_d.$$

The sequence of synthesis of controller algorithm based on the above will be as follows:

1. Inputs: parameters of control object, the transition process time in the projected system, controller discretization interval.
2. Achieving mathematical model of the object (7).
3. The transition to the discrete model (8).
4. Calculation of the auxiliary matrices (9).
5. Computation of feedback matrix K by solving the Riccati equation.
6. Selection of observer matrices A_n, B_n.
7. Calculation of the matrix C_n by solving Sylvester equation $C_n = lyap(A_n, -A_d, R_n C_d)$.
8. Calculation of the input observer matrix by control $B_n = C_n B_d$.
9. Calculation of the matrix N_1, N_2 according to (13).

Finally, the algorithm of the controller, after substituting (12) into (14), will have the form

$$w_{m+1} = (A_n + B_n N_2) w_m + (B_n N_1 + R_n) y_m$$
$$u_m = N_2 w_m + N_1 y_m$$

4 Modeling of system

In accordance with the above procedure of synthesis calculations of the algorithm parameters of the controller to a specific object with the location of the angle sensor as a first mass and a second mass were performed. This system consists of a digital drive signal generator, a discrete controller (9) and continuous object (7) in the case of the position sensor is located on the first mass [12] - [14].

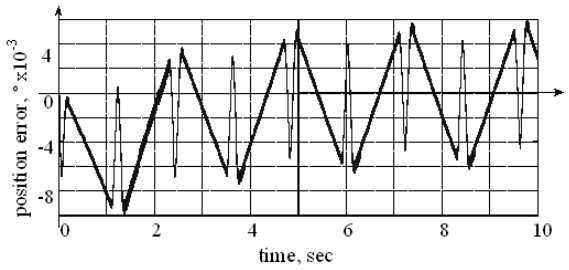

Figure 1. Position error of the second mass. Sensor is on the first mass.

Figure 1 shows a graph of position error of the second mass (actuator) when position sensor is installed on the first mass. The graph shows that the position error of the second mass in the work area does not exceed 0.0068 that is 1.2% of the maximum of position reference signal. There are oscillations with the amplitude of the second mass 0.00038 and period *T*, equal to the sampling period of the controller.

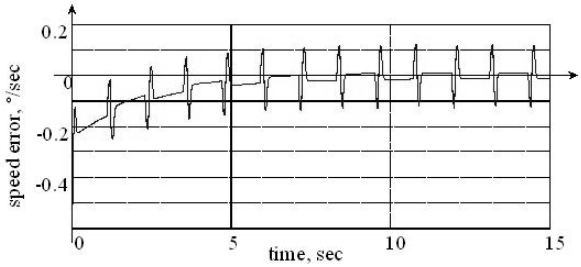

Figure 2. Speed error of the second mass. Sensor is on the first mass.

Figure 2 shows a graph of the speed error of the second mass (actuator) when position sensor is installed on the first mass. The graph shows that after the transient process is finished, speed error in the work area does not exceed 0.01 8/sec, which is 1% of the speed reference in the work area. It is clear from Figure 2, that process of is very long and speeding up of it can't be implemented due to saturation of the engine control unit.

When position sensor is installed on the second mass the higher level of quality of scanning system could be achieved. As an example, Fig. 3 shows a graph of the speed error of the second mass, when position sensor is installed on the second mass.

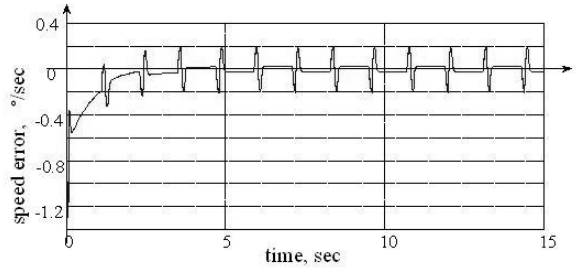

Figure 3. Speed error of the second mass. Sensor is on the second mass.

As can be seen from the graph, the transient process is significantly accelerated in this case [15], [16].

5 Conclusion

It could be said, that elasticity links are not critical for electromechanical scanner. It is only necessary to carry out the synthesis of controller algorithm using an object model that takes into account the elastic link.

The best results could be achieved when position sensor is installed on the second mass, directly on the actuator. This recommendation should always be used when design of electromechanical scanner allows the installation of the position sensor on the second mass. However, if it is not available, it is also possible to construct a working system, with only a few worse properties. The results obtained are recommended for use in high-precision electric drives of precision observations complexes.

6 Acknowledgement

This work was financially supported by Government of Russian Federation, Grant 074-U01.

References:

[1] Sarhan, H.S. , Issa, R.H., Alia, M.A., Al-Abbas, I.K. Precision speed control of DC motor drive system, *International Review of Automatic Control*, Volume 5, Issue 5, September 2012, pp. 673-676.

[2] Balkovoi, A.P., Kostin, A.V., Myagkikh, A.S., Tolstykh, O.A., Tsatsenkin, V.K., Yakovlev, S.F. Design of direct linear drives for manufacturing, *Russian Electrical Engineering*, 2013, Vol 7(84), pp. 363-369.

[3] Yu. P. Filyushov, V. Yu. Filyushov. Control of a synchronous machine under minimization of heat losses in conditions of minimal reactive power, *Russian Electrical Engineering*,

December 2013, Volume 84, Issue 12, pp. 712-717.

[4] Blaho, M., Bielko, S., Farkas, L., Fodrek, P. Computer based control with real-time capabilities. *WSEAS Transactions on Systems and Control*. Volume 9, 2014, pp. 16-27.

[5] S. G. Voronin, D. A. Kurnosov, A. S. Kul'mukhametova. Vector control of permanent-magnet synchronous motors, Russian Electrical Engineering, October 2013, Volume 84, Issue 10, pp. 581-585.

[6] Worthington, M.S., Beets, T.A., Beno, J.H., Mock, J.R., Murphy, B.T., Southa, B.J., Good, J.M. Design and development of a high precision, high payload telescope dual drive system, *Proceedings of SPIE - The International Society for Optical Engineering*, Vol. 7733, Issue PART 1, 2010.

[7] Ren, C., Liuzhao, Songlibin, Yiqiang, Chen, K., Zhang, Z. Design and simulation of the direct drive servo system, *Proceedings of SPIE - The International Society for Optical Engineering*, 2010.

[8] Tomasov V.S., Lovlin S.Ju., Tushev S.A., Smirnov N.A. Output voltage distortion of pulse width converter of precision electric drive, *Ivanovo: Vestnik IGEU*, Vol. 1, 2013.

[9] Sadovnikov Mikhail A., Tomasov Valentine S., Tolmachev Valery A., Precision Electric Drive for Optical Space Control Systems, *Scientific and Technical Journal «Priborostroenie»*, Vol. 54, No. 6, 2011, pp. 81-86

[10] Abbou, A., Nasser, T., Mahmoudi, H., Akherraz, M., Essadki, A. Induction motor controls and implementation using dSPACE. *WSEAS Transactions on Systems and Control*. Volume 7, Issue 1, 2012, pp. 26-35.

[11] Terec, R., Chindris, V., Szabo, L., Rafajdus. Position sensing system for switched reluctance motor control, *Proceedings of 9th International Conference, ELEKTRO 2012*, pp. 266-269.

[12] Chen, M.-Y. , Lu, J.-S. High-precision motion control for a linear permanent magnet iron core synchronous motor drive in position platform, *IEEE Transactions on Industrial Informatics* Volume 10, Issue 1, February 2014, Article number 6461410, pp. 99-108.

[13] Drozdov V.N., Tushev S.A. Ship motions influence on the range of possible coordinates of object observed by telescope on the deck, *Vestnik IGJeU*, Ivanovo 2013, Volume 4, pp. 54-58.

[14] Subbotin D.A., Lovlin S.Y., Tsvetkova M.H. Two-mass mathematical model of magnetoelectric converter for reversible scanning device. *Manufacturing Engineering, Automatic Control and Robotics: Proceedings of the 14th International Conference on Robotics, Control and Manufacturing Technology (ROCOM '14).* 2014, No. 32/1/1, pp. 11-14

[15] Subbotin D.A., Lovlin S.Y., Tsvetkova M.H. Identifying dynamic model parameters of a servo drive. *Manufacturing Engineering, Automatic Control and Robotics: Proceedings of the 14th International Conference on Robotics, Control and Manufacturing Technology (ROCOM '14).* 2014, No. 32/1/1, pp. 50-57

[16] Ahmed, A.H.O. High performance speed control of direct current motors using adaptive inverse control. *WSEAS Transactions on Systems and Control.* Volume 7, Issue 2, 2012, pp. 54-63.